Environment International 176 (2023) 107970

Contents lists available at ScienceDirect

Environment International

journal homepage: www.elsevier.com/locate/envint

Full length article

A spatial indicator of environmental and climatic vulnerability in Rome

Chiara Badaloni [a,*], Manuela De Sario [a], Nicola Caranci [c], Francesca de' Donato [a], Andrea Bolignano [d], Marina Davoli [a], Letizia Leccese [a], Paola Michelozzi [a], Michela Leone [b]

[a] Department of Epidemiology of the Lazio Regional Health Service, ASL Roma 1, Rome, Italy
[b] ASL Frosinone, Frosinone, Italy
[c] Regional Health and Social Care Agency, Emilia-Romagna Region, Bologna, Italy
[d] Lazio Environmental Protection Agency, Rome, Italy

ARTICLE INFO

Handling Editor: Xavier Querol

Keywords:
Environmental vulnerability
Climatic vulnerability
Social vulnerability
Geographically Weighted Principal Component Analysis
Composite indicator
Risk stratification

ABSTRACT

Background: Urban areas are disproportionately affected by multiple pressures from overbuilding, traffic, air pollution, and heat waves that often interact and are interconnected in producing health effects. A new synthetic tool to summarize environmental and climatic vulnerability has been introduced for the city of Rome, Italy, to provide the basis for environmental and health policies.

Methods: From a literature overview and based on the availability of data, several macro-dimensions were identified on 1,461 grid cells with a width of 1 km^2 in Rome: land use, roads and traffic-related exposure, green space data, soil sealing, air pollution ($PM_{2.5}$, PM_{10}, NO_2, C_6H_6, SO_2), urban heat island intensity. The Geographically Weighted Principal Component Analysis (GWPCA) method was performed to produce a composite spatial indicator to describe and interpret each spatial feature by integrating all environmental dimensions. The method of natural breaks was used to define the risk classes. A bivariate map of environmental and social vulnerability was described.

Results: The first three components explained most of the variation in the data structure with an average of 78.2% of the total percentage of variance (PTV) explained by the GWPCA, with air pollution and soil sealing contributing most in the first component; green space in the second component; road and traffic density and SO_2 in the third component. 56% of the population lives in areas with high or very high levels of environmental and climatic vulnerability, showing a periphery-centre trend, inverse to the deprivation index.

Conclusions: A new environmental and climatic vulnerability indicator for the city of Rome was able to identify the areas and population at risk in the city, and can be integrated with other vulnerability dimensions, such as social deprivation, providing the basis for risk stratification of the population and for the design of policies to address environmental, climatic and social injustice.

1. Introduction

The world population is growing rapidly, especially in developing countries, but also in industrialised countries, and the greatest burden will be in urban areas, with 2.8 billion more people by 2050 (United Nations, 2022a). This ongoing growth threatens the health of urban dwellers, especially the most vulnerable, due to multiple stressors such as air pollution, urban solid waste, extreme weather events, and inadequate public spaces and services, with actions to reduce such exposures still too slow and further delayed by the COVID-19 crisis, such that the United Nations Sustainable Development Goal of making cities and urban settlements more inclusive, safe, sustainable and resilient will be hard to achieve by the ever-closer 2030 (United Nations, 2022b). Cross-cutting urban stressors must be addressed to improve current and future urban health through actions such as urban planning, housing action plans, environmental policy and governance, sustainable transport and mobility, promoting nutritious food and increasing access to healthy diets, urban design to promote physical activity, strategies to manage pandemic such as COVID-19. This is a field where cooperation and knowledge sharing of solutions could make a difference as is the ambition of the WHO repository of Urban Health Resources (World Health Organization, 2022).

* Corresponding author at: Department of Epidemiology of the Lazio Regional Health Service ASL, Roma 1, Rome, Italy, Via Cristoforo Colombo, 112. 00147 Rome, Italy.
E-mail address: c.badaloni@deplazio.it (C. Badaloni).

https://doi.org/10.1016/j.envint.2023.107970
Received 14 February 2023; Received in revised form 14 April 2023; Accepted 8 May 2023
Available online 16 May 2023

Environmental hazards are often concentrated in urban areas, where some areas are disproportionately affected by the multiple pressures of urban waste, air pollution, industry, and extreme weather events, often interacting and interconnected in producing health effects (Kjellstrom et al., 2007). This is relevant from a descriptive perspective to characterise the vulnerability of the population, which is useful for planning and decision making, and from a research perspective, to analyse the health impacts of urban-related hazards in epidemiological studies. For both descriptive and analytical purposes, a finer spatial resolution allows for better insights. The possibility to studying environmental exposures has been exploited by spatial epidemiology in the last decade (Richardson et al., 2010, 2009), taking into account different exposures (e.g. climate, air pollution, industrial sites) and through openly available spatial resolution data (e.g. satellite data).

In recent decades, borrowing methods from the social sciences, even in epidemiology, especially for descriptive purposes, in order to respond the growing need for systematic information on complex realities, attempts to create synthetic and complex spatial indicators have multiplied. In general, these indicators have the advantage of reducing information from a large number of elementary variables in order to carry out simpler and faster analyses, especially in comparative terms. In epidemiology, both in Italy and in other countries, there is a solid evidence base of using synthetic spatial indicators in the field of socioeconomic inequalities, demonstrating the ability of social or deprivation indices to capture socioeconomic disadvantage linked to worse health outcomes, such as life expectancy even in old age (Cabrera-Barona et al., 2015; Cardoso-dos-Santos et al., 2018; Cesaroni et al., 2012; Lallo and Raitano, 2018; Lin et al., 2019; Marinacci et al., 2013; Padilla et al., 2016; Rosano et al., 2020; Samoli et al., 2019; Sartorius and Sartorius, 2014; Schuurman et al., 2007). It has been suggested that environmental exposures may contribute to amplifying health inequalities (Deguen and Zmirou-Navier, 2010; Slachtova et al., 2016). Although the health effects of individual environmental attributes (e.g. air pollution, traffic, noise) are well known (Dambha-Miller et al., 2022; Rojas-Rueda et al., 2021; Waidyatillake et al., 2021), only few attempts to derive environmental indices by analysing multiple environmental attributes simultaneously have been reported (Min et al., 2021; Ribeiro et al., 2015; Richardson et al., 2010, 2009; Saib et al., 2015). This synthesis is valuable in providing tools for decision makers to map and identify spatial injustice in urban areas due to multiple stressors on which to base integrated social, health and environmental prevention programs.

However, to inform and update the spatial dynamics of many environmental, social and economic processes together, is still rather challenging in terms of collecting reliable data for each relevant environmental dimension and in terms of heterogeneity of data availability and resolution in time and space (Degbelo and Kuhn, 2018). In a context such as Italy, the use of composite indices at the subnational level is particularly important in the analysis of the landscape inequalities that characterise our country, in terms of climate, land use, morphology/orography, north–south and rural–urban economic and industrial divide, both for an assessment of the current situation and to monitoring the evolution of the environmental and climatic vulnerability over time. Furthermore, environmental inequalities overlap with geographical differences in population ageing, health outcomes and determinants, and access to and quality of health and social care. In addition, a synthesis of spatial characteristics that integrates large amounts of information facilitates the understanding of the context in which people live.

To simplify the variety of the complex link between health and environmental/climatic vulnerability, one possibility is to develop a holistic approach by creating a new synthetic measure that captures the complexity of the urban landscape using fine resolution scales (Antrop, 2000). Since “everything is related to everything else, but the near things are more correlated than the far things” (Tobler, 2004, 1970), the spatial arrangement of observations must to be take into account. The standard multivariate exploration technique, such as principal component analysis (PCA) implicitly assumes that the correlation between indicators is constant in space (stationary), thus it is not a gold standard for spatially varying phenomena. For this reason, a variant of the PCA methodology, the Geographical Weighted Principal Component Analysis (GWPCA), has been proposed to describe the spatial effects of non-stationary phenomena. In general terms, GWPCA assumes that there are several regions in a given spatial domain in which different and distinct PCAs are to be applied. In this way, it is possible to consider the continuous variation of the results of the multivariate analysis in space. GWPCA makes it possible to assess the representativeness of the global PCA (standard) by providing a set of locally derived principal components at all data locations (Harris et al., 2011; Lloyd, 2010).

In this study, we introduce a composite indicator of environmental and climatic spatial vulnerability to describe and summarise the main environmental and climatic exposures in the municipality of Rome, capable of providing immediate and effective information to support the definition and implementation of environmental health policies.

2. Material and methods

2.1. Study area

Rome is the largest Italian city with a population of approximately 2.8 million inhabitants over an area of 1.290 km^2 (Italian National Statistics Institute, 2022). The city is characterised by a complex landscape with various anthropogenic and natural sources of air pollution. The urban landscape is very heterogeneous and it is therefore necessary to analyse small units in order to grasp the dynamic structure of the environmental exposures. For this purpose, we defined a common grid of 1,461 (1x1) km cells and used this as unit reference for all spatial predictors.

2.2. Selection of the environmental dimensions relevant for health in urban areas

To identify environmental factors associated to the health of people living in urban areas, an overview of reviews was carried out using three bibliographic databases (Medline, Embase, APA PsycInfo in OVID) from inception to 20 October 2022 (Appendix Part. A). From the 664 potentially eligible records after duplicated removal, 129 full texts were assessed for eligibility leading to 73 reviews published from 2015 to 2022 included in the narrative synthesis. The flow chart and the summary table are provided in the Appendix Part. B and Part. C, while the excluded reviews and those included after eligibility assessment of the full-text are reported in the Appendix Part. D. Overall, the review suggests that, in addition to socioeconomic factors, the most relevant environmental determinants of population health are air pollution, noise, temperatures, traffic density and built environment characteristics such as green spaces, and other neighborhood features (e.g., population density) which will be considered as main components environmental vulnerability index for Rome. More detailed results on the available evidence for specific urban-related risk and protective factors can be found in the Appendix Part. E.

2.3. Spatial data

From the previous literature overview, and taking into account the data availability for the city of Rome, several macro dimensions were identified for the present analysis which differ in terms of data source and spatial resolution (Table 1): land use (urban and rural); roads and traffic related exposure; green space data; impermeable cover of soil; air pollutants and urban heat island intensity. Each macro dimension is described through a set of spatial predictors rescaled at the grid cell level varying over space but not over time (Table 2).

Table 1
Description of the spatial data for the environmental vulnerability indicator of the city of Rome.

Environmental dimension	Description	Source	Original Spatial resolution
Land use data	Land cover characteristics (urban and rural area)	Corine Land Cover 2018 https://www.sinanet.isprambiente.it	scale 1:100.000
Roads and traffic related exposure	Roads based on CLC Functional Road Classification (FRC 0:5) (type: highway, major, secondary, or local road)	TeleAtlas TomTom (2015)	metres
	Daily vehicles per hour in the rush hour	Urban traffic plan of Rome municipalities (2009)	road arch
	Noise traffic level estimate at each 5 m along the façade of the buildings in which subjects lived	Ascari et al. 2017	point (coord (lat,long))
Green space data	Urban green space area (type:land use, leisure,natural and biopark)	OpenStreetMap (2019)	areal (m^2)
	Normalised Difference Vegetation Index (NDVI)	MODIS NDVI (MOD12A3) (2015)	(1x1) km
	Leaf Area Index (LAI)	Image of Landsat 8 (2015)	(30x30) m
Impermeable cover of soil	Soil Sealing Index	https://land.copernicus.eu/pan-european/high-resolution-layers/imperviousness/status-maps/2015/view	(100x100) m
Air pollution	$PM_{2.5}$, PM_{10}, NO_2, C_6H_6, SO_2	FARM model (2018)	(1x1) km
Urban Heat Island	UHI: Urban heat island intensity summer 2001-2010	Air temperature derived from spatiotemporal models.	(1x1) km

Table 2
Description of the spatial predictors for the environmental vulnerability indicator of the city of Rome.

Environmental dimension	Indicators
Land use data	% Urban use
	% Rural use
Roads and traffic related exposure	Road density (m/m^2)
	Traffic density (daily vehicels per cubic metre)
	Traffic noise (dBA)
Green space data	% Urban green space area
	NDVI dimensionless, values from −1 to + 1
	LAI dimensionless, positive values
Impermeable cover of soil	% Soil Sealing Index
Air pollution	$PM_{2.5}$ ($\mu g/m^3$)
	PM_{10} ($\mu g/m^3$)
	NO_2 ($\mu g/m^3$)
	C_6H_6 ($\mu g/m^3$)
	SO_2 ($\mu g/m^3$)
Urban heat island	Urban heat island intensity (°C)

2.3.1. Land use data:

We characterised each cell (1×1) km in terms of land cover classes based on the Corine Land Cover (CLC) (Italian National Institute for Environmental Protection, 2018). The CLC is a map of the European environmental landscape based on the interpretation of satellite images. It provides comparable digital land cover maps for each country and for large parts of Europe, with spatial resolution of (250×250) m. We used the following spatial predictors:

a. Percent urban development area. We selected two CLC classes (high/low development) and of each cell (1x1) km, we computed the percentage covered by an area of urban development.
b. Percent rural development area. We selected several CLC classes (arable land, crop, pasture, agriculture, deciduous, evergreen, shrub) and of each cell (1x1) km, we computed the percentage covered by an area of rural development.

2.3.2. Roads and traffic-related exposures

a. Road density. We collected road density information from the TeleAtlas TomTom (2015) road network (FRC 0–5), by selecting highway, major road, secondary road, or local road according to the Functional Road Classification (FRC). For each class and each grid cell (1×1) km, we calculated the number of metres (as the sum of all segments) within the cell.
b. Traffic density. We collected road traffic data provided by the Mobility Agency of Rome for all major roads for 2009. Road traffic data were representative of the rush hour and reported per arch (segment direction) (i) the number of passenger car equivalent (PCE) vehicles per hour, (ii) average speed during rush hour, and (iii) traffic model parameters (capacity, alpha/beta). We characterised the traffic density for each grid cell (1×1) km as the number of cars multiplied by the length of roads within the cell divided by the cell's area.
c. Traffic noise. We collected road traffic data as described above for the traffic density predictor. Noise estimates were calculated using the method from the German VBEB standard (Germany Federal Environment Agency, 2007). The method was applied to provide noise estimates each 5 m along the façade of residential buildings (Ascari et al., 2017). The cell-level noise estimate was obtained by averaging the energy of the point estimates of the building façade contained in the cell. As noise metrics, we calculated annual day-evening-night A-weighted equivalent continuous noise levels (Lden) and Lnight for the hours 22:00 – 06:00. Each indicator gives an A-weighted decibels (dBA) level as an expression of the relative loudness of sounds in air as perceived by the human ear.

2.3.3. Green space data

a. The Open Street Map (OSM) (The Open Knowledge Foundation, 2023) information was downloaded, and the following macro areas were selected: land use, leisure, natural and biopark. A specific shapefile with parks and gardens was built. The percentage of each cell covered by a green area was used as a predictor of green.
b. Normalised Difference Vegetation Index (NDVI) in 2015 was used. We collected the available monthly MODIS NDVI product (MOD13A3) at (1×1) km spatial resolution.
c. Leaf Area Index (LAI) in 2015 was used. The index is a dimensionless variable given by a ratio of leaf area to per unit ground surface area; this value was used as an important vegetation biophysical parameter.

2.3.4. Impermeable cover of soil

The Soil Sealing Index provides information on land cover with impermeable material that often compromises fertile agricultural land, endangers biodiversity, increases the risk of flooding and water scarcity and contributes to global warming. Soil sealing estimates the increase in soil surfaces sealed with impervious materials due to urban development and construction (such as buildings, constructions and the laying of completely or partially impermeable artificial material, such as asphalt, metal, glass, plastic or concrete). This provides an indication of the rate

of soil sealing, which occurs when areas change use to artificial and urban land use.

2.3.5. Air pollution

The following air pollutants (PM_{10}, $PM_{2.5}$, NO_2, C_6H_6, SO_2) were estimated using the Flexible Air quality Regional Model (FARM) for year 2018. FARM is a three-dimensional Eulerian model that accounts for transport, chemical evolution and deposition of atmospheric pollutants (Chang et al., 1987).

2.3.6. Urban heat island

From multivariate spatiotemporal models, daily mean air temperature at a (1x1) km resolution was estimated from MODIS land surface temperature (LST) satellite data, temperature observations provided by monitoring networks, and spatial and spatiotemporal land use variables (de'Donato et al., 2018). From the (1x1) km data, the average temperature for each cell over the period 2001–2010 was defined and the urban heat island intensity (UHI) for Rome was defined as the difference between temperatures in each grid cell and the coolest cell located in the rural surroundings within the Rome municipality study domain (de'Donato et al., 2018).

2.4. Deprivation index

Given the substantial contribution of socio-economic dimension on population health in urban areas as confirmed by the previously mentioned reviews (Akinyemiju et al., 2015; Besser et al., 2017; Beyer et al., 2015; Johnson et al., 2019; Salgado et al., 2020; Soffian et al., 2021; Sui et al., 2022) and considering the potential effect modification of environmental exposure effects, to capture the relationship between the environmental data and the socioeconomic status we used a synthetic deprivation index (Rosano et al., 2020) built using individual data from the 2011 General Population and Housing Census (Italian National Statistics Institute, 2011). The multidimensional concept of social and material deprivation was summarised combining indicators of five characteristics at the census tract level: low education level, unemployment status, single parent household, rented and high-density housing. The index consists in the sum of standardised indicators; it grows with social and material disadvantage and its continuous value was scaled from census tract to grid cell resolution.

2.5. Environmental and climatic vulnerability composite spatial indicator

The Geographically Weighted Principal Component Analysis (GWPCA) method was used to produce a composite spatial indicator by integrating the environmental and climatic dimensions described above.

This method is an extension of standard Principal Component Analysis (PCA) and was performed to account for spatial heterogeneity. Although the standard PCA analysis can provide information on the global internal structure, it cannot account for the fact that the covariance structure of the data can change spatially (Tejedor-Flores et al., 2020). However, both analyses were implemented. Standard PCA was used to reveal globally which components have eigenvalues greater than or very close to unity and the proportion of the variation in the data, then GWPCA was applied to reduce the size of the dataset (in terms of number of variables) by transforming the original set into a new set of uncorrelated variables using local covariance decomposition.

Briefly, as a spatial multivariate technique, GWPCA takes into account non-stationarity of the spatial process (Harris et al., 2011) and is able to pursue several objectives: investigating spatial heterogeneity in the structure of multivariate data, calibrating the model, assessing how data dimensionally varies spatially (eigenvalue) and how the original variables influence each spatially varying component (eigenvectors), and reducing the dimensions of the data set (in terms of number of variables) into a new set of uncorrelated variables (Gollini et al., 2015). The statistical analysis was carried out in four steps described below.

2.5.1. Step.1

The first step was to verify the spatial non-stationarity. In order to diagnose the possibly presence of spatial non-stationarity or specifically whether the geographically weighted eigenvalues of the GWPCA vary significantly in space, the Monte Carlo test was conducted on a large number of randomised distributions (in our case 99). Moreover, univariate spatial autocorrelation, a measure of spatial units clustering, was tested globally for all spatial predictors. In the absence of spatial autocorrelation, the spatial allocation of observations can be assumed to be random. The Moran's *I* estimator was used.

2.5.2. Step.2

The second step was to calibrate the model. The bi-square kernel function was used to calibrate the model. This function assigns null weights to observations with a distance greater than a determined bandwidth found through the cross-validation procedure. The cross-validation score was calculated for all possible bandwidth selections, and the optimal one was the bandwidth showing the lowest cross validation score (Gollini et al., 2015).

2.5.3. Step.3

Once the bandwidth was chosen, GWPCA analysis was performed. This technique implements a different principal component model at each location with a geographically weighted subset of neighbouring data points and computes a new set of variables to account the majority

Table 3
Descriptive statistics of spatial indicators for the environmental vulnerability indicator of the city of Rome.

Environmental dimension	Indicator	Mean	SD	Percentiles				
				5°	25°	50°	75°	95°
Land use data	% Urban use	22.4	31.7	0	0	0.5	40.5	92
	% Rural use	67.6	36	0	37.8	84.3	99.9	100
Roads and traffic related exposure	Road density (m/m^2)	0.002	0.002	0	0.001	0.002	0.003	0.007
	Traffic density (daily vehicles per cubic metre)	29.4	43	0	2.1	10.2	38.8	127.3
	Traffic noise (dBA)	54.7	11.4	33	48.3	57.1	63.2	68.6
Green space data	% Urban green space area	48.9	39	0.5	9.3	43.3	94.6	100
	NDVI	0.5	0.1	0.3	0	0.5	0.6	0.7
	LAI	3.6	0.9	2.5	3	3.5	4.2	5.4
Impermeable cover	% Soil Sealing Index	15	18.8	0	0.9	5.4	25.6	54.3
Air pollution	$PM_{2.5}$ ($\mu g/m^3$)	13.2	2.7	9.6	10.9	12.9	15.3	18.2
	PM_{10} ($\mu g/m^3$)	18.1	4.2	12.3	14.6	17.6	21.3	25.9
	NO_2 ($\mu g/m^3$)	27.2	12.9	10	17.1	24.2	37.6	50.1
	C_6H_6 ($\mu g/m^3$)	0.9	0.4	0.4	0.6	0.8	1.1	1.7
	SO_2 ($\mu g/m^3$)	2.3	1.1	1.3	1.7	2	2.6	3.7
Urban heat island	UHI (°C)	1.6	0.6	0.6	1.4	1.6	2	2.6

SD: standard deviation.

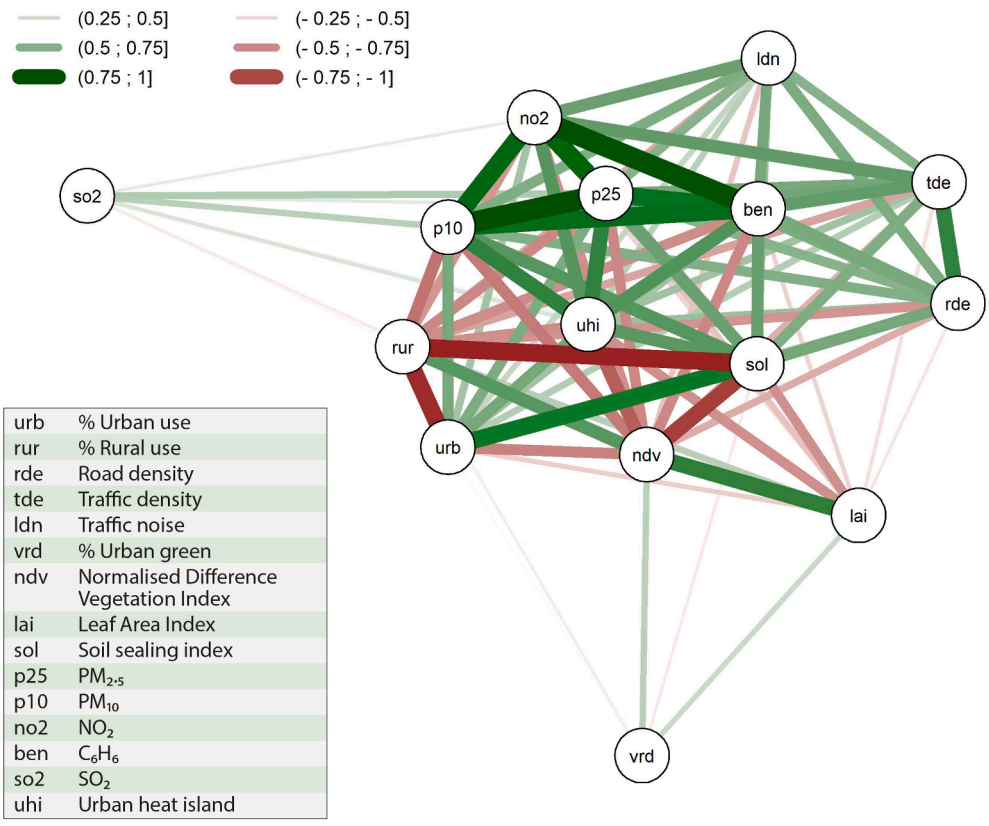

Fig. 1. The correlation network plot of environmental predictors for the environmental vulnerability indicator of the city of Rome.

Table 4
Summary of standard PCA results.

	Component 1	Component 2	Component 3
Importance of components			
Proportion of Variance explained	56.9%	11.1%	7.4%
Cumulative Proportion of variance explained	56.9%	68.0%	75.3%
Loadings			
% Urban use	0.258	0.208	0.165
% Rural use	0.275	0.202	0.172
Road density	0.252	−0.098	0.398
Traffic density	0.254	−0.16	0.316
Traffic noise	0.229	−0.228	0.296
% Urban green	0.092	0.538	0.128
NDVI	0.275	0.333	−0.118
LAI	0.204	0.4	−0.255
Soil Sealing Index	0.298	0.211	0.119
$PM_{2.5}$	0.303	−0.217	−0.214
PM_{10}	0.311	−0.182	−0.176
NO_2	0.295	−0.276	−0.056
C_6H_6	0.297	−0.251	−0.057
SO_2	0.142	−0.056	−0.596
UHI	0.283	0.03	−0.223

of information about the original data. The eigenvalues reflect the variance explained by each component for each cell and were used to select the necessary number of components. The loadings reflect the spatial (local) importance of the variables, the extent of association and co-variability.

The interpretation of the GWPCA results was supported with the visualisation method proposed by Harris et al. by mapping the proportion of the variance explained by the principal components, and the winning variable of each PC and using multivariate glyphs to represent the loadings at all locations (Harris et al., 2011).

The GWPCA method has been performed in the R platform using the GWmodels Package (Gollini et al., 2015; Lu et al., 2014).

2.5.4. Step.4

The natural breaks method was used to define eleven classes of risk, the first six levels identify a very low level of vulnerability, while the last five classes describe the level of vulnerability from the lowest to the highest vulnerability.

2.6. Bivariate association with deprivation index

The bivariate choropleth map was used to identify the spatial relationships and patterns between vulnerability and deprivation index. Each indicator was grouped into three classes: low, medium and high. The indicator identified very low vulnerability as class 1, low, medium low and medium high as class 2, while high and very high vulnerability as class 3. The deprivation index was aggregated as follow: low and medium low as class 1, medium and medium high as class 2 and high as class 3.

The number of inhabitants exposed to these levels of environmental and climatic vulnerability and the distribution by deprivation status was described.

To investigate how the association changed over space and to capture bivariate spatial association among the vulnerability index and the deprivation index, Lee's *L* statistical measure were calculated (Lee, 2001). In this context, the commonly used Pearson's correlation coefficient does not capture the spatial distribution dimension of the two geographical variables. Our interest was to evaluate whether the bivariate associations were spatially clustered. The *L* index sums up two aspects of spatial correlation: first, the relationship within a pair of geographical variables at each location (in terms of point-to-point association); second, the relationship between distinct pairs across locations (in terms of spatial association). The local *L* index was used to

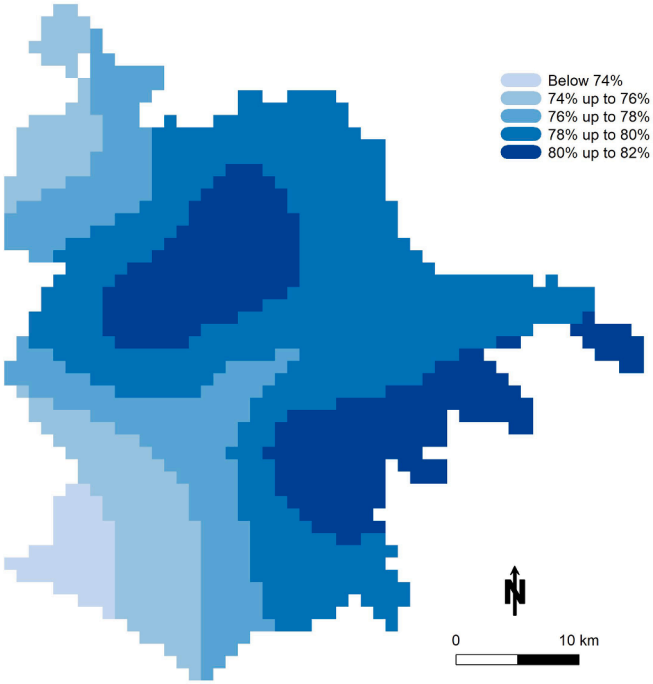

Fig. 2. Spatial variation in the amount of variance explained by the first three components from GWPCA.

create a map and discern sub-regions into the four categories: high-high and low-low locations (spatial clusters) and high-low and low–high locations (spatial outliers).

3. Results

The Figs. (1 to 16) in the Appendix Part. F displays the spatial distributions in exposure of all environmental input variables, while Table 3 shows the descriptive statistics of spatial indicators used to build the vulnerability index.

Fig. 1 describes the correlation network between spatial predictors, green lines showing the positive correlation, red lines negative correlation and the thickness documenting the magnitude of the correlation. Traffic-related air pollutants, as PM_{10} (p10), $PM_{2.5}$ (p25), NO_2 (no2), C_6H_6 (ben), are highly correlated with each other, while SO_2 (so2) (industrial-related pollutant) is less correlated and far from the other pollutants. On the contrary, the green predictors like NDVI (ndv), LAI (lai) and urban green (vrd) are negatively related with air pollution and also negatively correlated with soil sealing.

The spatial non-stationarity was tested with a Monte Carlo test (Fig. 1 in Appendix Part. F), specifically to verify whether the geographically weighted eigenvalues of the GWPCA varied significantly in space. The observed p-value of the local eigenvalues of the GWPCA is 0.03, therefore it is reasonable to reject (at the 95% level) the spatial invariance hypothesis of the local eigenvalues, confirming a certain degree of spatial non-stationarity in the spatial predictors of environmental vulnerability.

The spatial positive autocorrelation was tested for all dimensions with the Moran's I (p-value $\sim$ 0) (Table 1 in Appendix F).

The calibration of the GWPCA model was performed using the bi-square kernel function. Particularly, the optimal adaptive bandwidth of 903 units was automatically found through a 'leave-one-out' cross-validation (CV) approach.

Once the non-stationarity was tested and the bandwidth had been chosen, PCA and GWPCA analysis were performed. Standard PCA reveals that the first three components collectively account for 75.3% of the variation in the data (Table 4). The loadings distribution suggests an interpretation of each component. Component 1 appears to represent air pollution, mainly PM_{10} and Soil Sealing Index; component 2, green space areas and component 3, industrial air pollution (SO_2) and road and traffic-related exposures. The PCA statistics and interpretations refer to the whole Rome municipality (Gollini et al., 2015) and represent an average value, which may not reliably show the local data structure of each km^2.

Fig. 2 represents the spatial distribution of the local percentage of variance explained by the first three principal components of the GWPCA. The total percentage of variance (PTV) explained ranges from 71.8% to 81.7% with an average value of 78.2%.

In general, the percentage of variance explained in the GWPCA is higher than the percentage of variance explained in the standard PCA (75.3%). Fig. 2 shows a geographical variation in the local percentage of explained variance, with the higher percentages ($\sim$80%) located in the northern areas and the lowest percentages (below 74%) located in the south-western areas (in the seaside area).

To investigate how the original variables influence each spatially varying component (eigenvectors), we mapped the highest absolute local (in each km^2 pixel) loadings (winning variables) into each of the three geographically weighted principal components (Fig. 3 a-b-c). The winning variables suggest which are the most important variables influencing the final indicator. For example, in the map a) the dark blue area indicates the (1x1) km pixels where soil sealing was the winning variable in the first component of the local GWPCA.

The visualisation maps of the winning variables for the three GWPCA components provide information on the influence of spatial spread in the study area, confirming the urban characterisation of Rome, with different variables affecting different parts of the city (Harris et al., 2011).

The environmental vulnerability composite spatial indicator has been visualised in Fig. 4 as a map resulting from the GWPCA model. The synthetic value of the indicator captures the spatial variability of the territory, highlighting the areas of greatest urban-related hazards in the city of Rome. The map shows greater environmental and climatic vulnerability in the city centre, with a decreasing gradient of vulnerability from the centre to the periphery.

Table 5 describes the percentage of the resident population (of all ages) exposed to different levels of the environmental and climatic

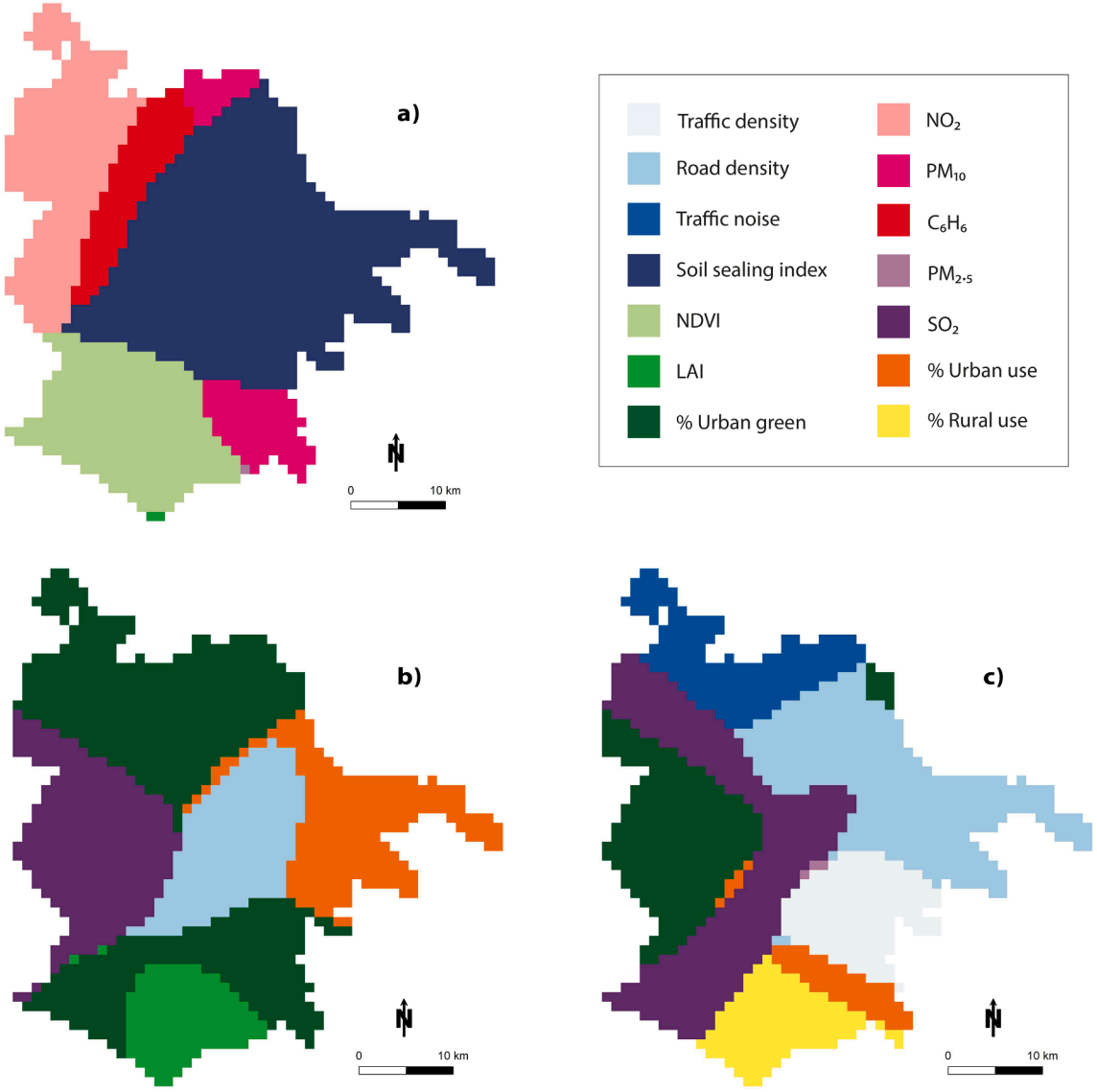

Fig. 3. The winning variables: the highest absolute loading on local Component 1(a) Component 2(b) Component 3(c) of the GWPCA.

vulnerability composite spatial indicator. The first six levels (from 1 - dark blue to 6 - grey) identify very low level of vulnerability, while the next five levels (from 7 - light purple to 11 - dark purple) describe five classes of vulnerability from low to very high. The majority of residents (56%) live in areas with high or very high levels of environmental and climatic vulnerability.

The proportion of the population exposed to the environmental vulnerability by deprivation level (Table 6) highlights an inverse pattern, with a larger share of the deprived population in lower environmental and climatic vulnerability levels, and viceversa, a higher fraction of the population exposed to higher environmental and climatic vulnerability levels in low deprivation areas. Overall, 13% of population with high deprivation lives in areas at very high risk for environmental and climatic vulnerability.

The bivariate choropleth maps (Fig. 5) visualise the spatial relationship between environmental and climatic vulnerability and deprivation. Low deprivation is represented by light (low) to dark (high) values of a red hue, while environmental and climatic vulnerability is represented by light (low) to dark (high) values of a purple hue. The resulting matrix of mixed colours identifies areas with high levels of both indices, low levels of both indices, and areas with all the other combinations of the two mapped indices (low-medium, low–high, medium–low, medium-medium, medium–high, high-low, high-medium). Fig. 5 suggests the presence of spatial clusters with both environmental and social vulnerability in eastern area of Rome, and in the western area (the Pisan area) and towards Malagrotta. The eastern areas are confirmed as spatial cluster for both indicators according to the L statistic (Lee) (Figure 18 in Appendix Part. F).

4. Discussion

Urban areas are locations of strong anthropic pressures on climate, soil, air, water and ecosystems producing multiple environmental exposures such as air pollution, traffic noise, heat waves, lack of green space, urbanicity. All these hazards, often interacting with each other, may have a number of adverse health effects with stronger evidence on cancer and on cardiovascular, metabolic and respiratory outcomes in both the general population and on specific vulnerable groups, but there is also emerging evidence on pregnancy outcomes, mental health, cognitive and behavioral problems in children, and cognitive decline among the elderly (Achilleos et al., 2017; An et al., 2018; Attademo et al., 2017; Babadjouni et al., 2017; Bernardini et al., 2020; Dendup et al., 2018; Jia et al., 2021; Lam et al., 2021; Li et al., 2016; National Toxicology, 2019; Rojas-Rueda et al., 2021; Rugel and Brauer, 2020;

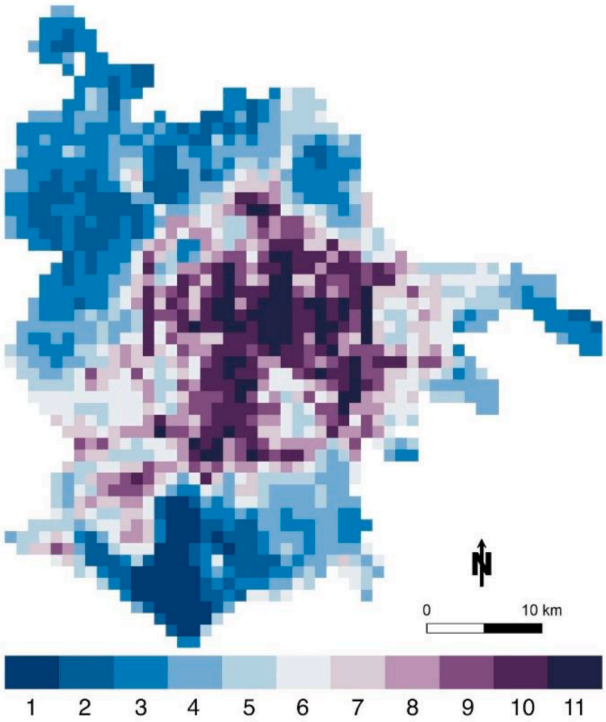

Fig. 4. The environmental and climatic vulnerability composite spatial indicator of the city of Rome. Legend shows categories of environmental vulnerability index (natural breaks) from low (1 - dark blue) to high (11 - dark purple). (For interpretation of the references to colour in this figure legend, the reader is referred to the web version of this article.)

Table 5
The population distribution by environmental and climatic vulnerability composite spatial indicator.

Environmental and climatic Vulnerability indicator	% of population exposed	Cumulative %
Very low	10%	10%
Low	8%	18%
Medium low	12%	30%
Medium high	14%	44%
High	33%	77%
Very high	23%	100%

Table 6
The percentage of population exposed to environmental and climatic vulnerability by deprivation level.

Deprivation indicator	Vulnerability environmental and climatic indicator					
	Very low	Low	Medium low	Medium high	High	Very High
1: low	8.3%	18.3%	13.6%	12.3%	24.8%	24.5%
2	14.9%	15.6%	26.9%	22.0%	18.1%	23.0%
3	17.9%	16.9%	23.3%	16.3%	18.6%	26.5%
4	30.8%	22.4%	18.4%	28.2%	20.1%	12.9%
5: high	28.1%	26.8%	17.8%	21.2%	18.3%	13.2%
	100%	100%	100%	100%	100%	100%

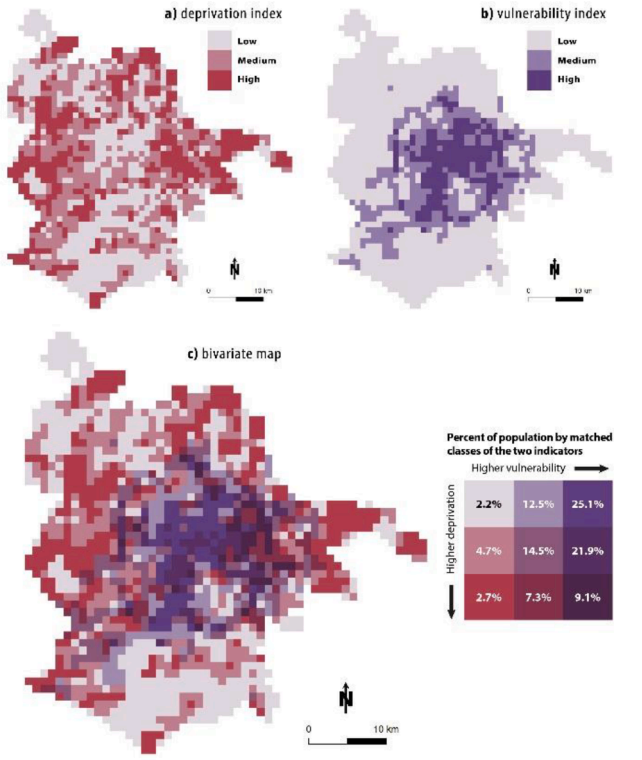

Fig. 5. Bivariate map between environmental and climatic vulnerability and deprivation indicators.

Salgado et al., 2020; Stieb et al., 2020; Vilcassim et al., 2021; Waidyatillake et al., 2021; Wimalasena et al., 2021; Yang et al., 2021; Zhu et al., 2020).

In this context, a summary measure of environmental vulnerability is able to capture not only the effect of single exposures, but also the combined risk perhaps greater than the sum of all contributing hazards. This study has developed and calibrated a new vulnerability and climatic indicator for the city of Rome that appears to be able to capture the complex interactions between exposures across space, exploiting advanced statistical techniques namely the Geographically Weighted Principal Component Analysis. With almost 60% of the resident population classified as living in high and very high vulnerability areas, the indicator identifies the most vulnerable areas to be prioritized with policies that address environmental inequalities. The fine spatial resolution of (1x1) km allows for a lower spatial unit than commonly considered, i.e. census tract, district, and reduce the magnitude of the misclassification error in attributing spatial exposures to the individual level. As expected, the highest environmental and climatic vulnerability is found in the city centre, where the urban heat island effect, traffic and noise pollution, soil imperviousness and lack of green spaces are greatest, but there are also clusters of risk in the western part of the city, near the landfill of Malagrotta, and in the industrial corridor in the eastern part of the city, already recognized as highly polluted areas and related to a higher mortality risk (Cesaroni et al., 2013; Michelozzi et al., 1998).

It is worth considering that urban-related environmental exposures have a number of adverse effects on the resident population as consistently showed by the overview of reviews (Achilleos et al., 2017; An et al., 2018; Attademo et al., 2017; Babadjouni et al., 2017; Bernardini et al., 2020; Dendup et al., 2018; Dzhambov and Dimitrova, 2018; Jia et al., 2021; Lam et al., 2021; Li et al., 2016; National Toxicology, 2019; Rojas-Rueda et al., 2021; Rugel and Brauer, 2020; Salgado et al., 2020; Stieb et al., 2020; Tortorella et al., 2022; Vilcassim et al., 2021; Waidyatillake et al., 2021; Wimalasena et al., 2021; Xu et al., 2018, 2016; Yang et al., 2021; Zhu et al., 2020). In particular green spaces may reduce the risk of maternal and child-related outcomes (Akaraci et al., 2020; Hu et al., 2021; Islam et al., 2020; Lee et al., 2020; Luque-Garcia et al., 2022; Nguyen et al., 2021; Vanaken and Danckaerts, 2018; Ye et al., 2022; Zhang et al., 2022) and of chronic diseases (Chen et al., 2022; De la Fuente et al., 2021; DenBraver et al., 2018; Dendup et al., 2018; Geneshka et al., 2021; Islam et al., 2020; Kabisch et al., 2017; Lam et al., 2021; Mmako et al., 2020; Nguyen et al., 2021; van den Bosch and Ode Sang, 2017; Ye et al., 2022; Zhang et al., 2022), and improve mental

health (Bonaccorsi et al., 2022; Bray et al., 2022; Kabisch et al., 2017; Sokale et al., 2022; van den Bosch and Ode Sang, 2017; Vanaken and Danckaerts, 2018; Zhang et al., 2022) and general wellbeing (Bogar and Beyer, 2016; Bonaccorsi et al., 2022; Nguyen et al., 2021; Padeiro et al., 2022; Zhang et al., 2022). This large body of evidence confirms that health impacts and potential benefits are greatest among vulnerable groups, such as children and adolescents, the elderly, people with chronic diseases or those living in deprived areas with limited resources. Moreover, there is a complex interplay between environmental and socioeconomic factors that represent another key risk factor for health in urban areas (Akinyemiju et al., 2015; Besser et al., 2017; Beyer et al., 2015; Johnson et al., 2019; Salgado et al., 2020; Soffian et al., 2021; Sui et al., 2022).

In the present study, the environmental and climatic vulnerability indicator seems to be complementary to the deprivation index (Rosano et al., 2020), whereby in Rome the social deprivation follows an inverse centre-periphery trend, this the opposite trend compared to the environmental vulnerability. The bivariate map of the two risks therefore adds new insights for the identification of the vulnerable population, with clusters of both risks in some eastern and western areas of the city, being the basis for guiding policies addressing both vulnerabilities.

With the aim to build an increasingly sensitive tool, the environmental and climatic vulnerability indicator is a flexible tool that can be extended to include additional environmental exposures. Moreover, to support public health policies, as exemplified by the social-environmental vulnerability bivariate analysis, our index can be integrated with data on health outcomes, health risk behaviours, prevention interventions, by providing a risk stratification tool of the population and representing a potentially interactive and open source data tool for population-level analysis and community estimates of health measures at different spatial level (municipality, city district, census tracts, and zip code) such as the PLACE dashboard of the US CDC (US CDC, 2022). Thanks to public availability of many environmental data, this tool could be replicated to all urban areas of Lazio region (Cartone and Postiglione, 2021) where there is a novel interactive open data tool on health outcomes (https://www.opensalutelazio.it/) (Lazio Region and Department of Epidemiology of Lazio Region, 2023) in which the environmental vulnerability and climatic indicator could be integrated, and it could also be replicated in other areas of Italy. Moreover, considering the clusters of vulnerability in areas of the city characterized by severe industrial pressure, if air dispersion modelling data from main industrial sites become available, this may be another area of improvement of the vulnerability indicator. Another potential development of the tool is the possibility to carry out etiological studies on health outcomes in different life stages, using the birth cohort PiccoliPiù (Farchi et al., 2014) and the longitudinal Rome study data (Cesaroni et al., 2012) that are enriched by an amount of individual characteristics which are modifiers or mediators of the exposure-health associations.

We proposed Geographically Weighted Principal Component Analysis (GWPCA) to reduce the dimensionality of the data and to capture the maximum information present in the original spatial phenomena. This technique allows to capture the spatial variability of the data better than standard PCA, allowing for a greater percentage of explained variance (78.2%-GWPCA vs 75.3%-PCA). In spatial analysis, according to Tobler's first law of geography (Tobler, 2004, 1970), understanding the geographical variation of environmental dimensions is of clear importance to support policy planning for environmental health. As spatial data, all sets of indicators vary locally and have a location (x,y) associated with each measurement, as they contain information on geographical position and environmental dimensions (Demšar et al., 2013). Therefore, attributes in some locations tend to be related among each others (Demšar et al., 2013). These two properties, called spatial heterogeneity and spatial autocorrelation, drive the inclusion of a geographical dimension in our analysis and suggest the need to exploit a variant of the standard PCA methodology. The GWPCA includes information on spatial heterogeneity and captures the spatial effects of non-stationary phenomena. In general terms, GWPCA assumes that in a given spatial domain there are several regions where different and distinct PCAs are to be applied. This makes it possible to consider the continuous variation of results in space. The GWPCA allows the representativeness of the standard PCA to be assessed by providing a set of locally derived principal components for all data locations (Harris et al., 2011; Lloyd, 2010). Thus, the final environmental and climatic vulnerability composite indicator depends on local environmental circumstances and the variables are weighted differently according to their significance for each grid cell. Therefore, the GWPCA index displays a sum of different phenomena and compares the values across space, where each grid cell is related to its neighbouring cells.

Despite synthetic environmental and climatic vulnerability indicator represent a unique opportunity to provide easy-to-read information to policy makers and have the added value to taking into account several exposures at the same time, there are some challenges. One aspect is the interpretation of data values that result from complex statistical reshaping of data and are dimensionless. Another issue is the heterogeneity of the original data in terms of period, spatial resolution and data source, with each variable affected by a specific measurement error. Regarding the interpretability of the combined indicator values, it is important to note that the GWPCA technique compared to standard PCA allows for a better interpretation of data through the use of the winning variables that support the characterization of the local city structure, with different variables dominating in different areas, as suggested by Harris (Harris et al., 2011). Another critical aspect concerns the potential misclassification bias in the attribution of spatial exposure at the individual level by linking the vulnerability indicator to residential address that could be affected by errors in the geolocation and in the information of address available in the population archives (Delmelle et al., 2022).

In conclusions, the study demonstrates the feasibility of developing a combined environmental and climatic vulnerability tool in the city of Rome, one of the largest urban areas in Europe, characterised by a wide range of different landscapes and multiple environmental stressors. The tool has enabled the identification of at risk areas and population subgroups in the city and can be integrated with other vulnerability dimensions, such as social deprivation, providing the basis for risk stratification of the population and the design of policies to address environmental and social injustice. Future advancements of the tool include integration with health data and other risk factors (e.g. lifestyle) and the extension of the indicator to other areas of the Lazio region and the entire country could be envisaged.

CRediT authorship contribution statement

Chiara Badaloni: Conceptualization, Methodology, Formal analysis, Writing – original draft, Writing – review & editing. **Manuela De Sario:** Investigation, Writing – original draft, Writing – review & editing. **Nicola Caranci:** Resources, Data curation. **Francesca de' Donato:** Resources, Data curation. **Andrea Bolignano:** Resources, Data curation. **Marina Davoli:** Supervision, Validation. **Letizia Leccese:** Software, Visualization. **Paola Michelozzi:** Conceptualization, Supervision, Validation. **Michela Leone:** Conceptualization, Writing – original draft, Writing – review & editing.

Declaration of Competing Interest

The authors declare that they have no known competing financial interests or personal relationships that could have appeared to influence the work reported in this paper.

Data availability

Data will be made available on request.

Acknowledgements

Authors would like to thank Simona Ricci for her support in graphic design and Patrizia Compagnucci for her help in articles retrieval for the literature overview. Project carried out with the technical and financial support of the Ministry of Health – PNC "Cobenefici di salute ed equità a supporto a supporto dei piani di risposta ai cambiamenti climatici in Italia" and of the HORIZON 2020 ENBEL Project no. 101003966 – ENBEL - 422 H2020-LC-CLA-2020-1.

Appendix A. Supplementary material

Supplementary data to this article can be found online at https://doi.org/10.1016/j.envint.2023.107970.

References

Achilleos, S., Kioumourtzoglou, M.-A., Wu, C.-D., Schwartz, J.D., Koutrakis, P., Papatheodorou, S.I., 2017. Acute effects of fine particulate matter constituents on mortality: A systematic review and meta-regression analysis. Environ. Int. 109, 89–100. https://doi.org/10.1016/j.envint.2017.09.010.

Germany Federal Environment Agency, 2007. VBEB, Preliminary calculation method for determining the number of environmental noise loads [VBEB, Vorläufige Berechnungsmethode zur Ermittlung der Belastetenzahlen durch Umgebungslärm]. Nicht amtliche Fassung der Bekanntmachung im Bundesanzeiger 75.

Akaraci, S., Feng, X., Suesse, T., Jalaludin, B., Astell-Burt, T., 2020. A systematic review and meta-analysis of associations between green and blue spaces and birth outcomes. Int. J. Environ. Res. Public Health 17, 2949. https://doi.org/10.3390/ijerph17082949.

Akinyemiju, T.F., Genkinger, J.M., Farhat, M., Wilson, A., Gary-Webb, T.L., Tehranifar, P., 2015. Residential environment and breast cancer incidence and mortality: A systematic review and meta-analysis. BMC Cancer 15, 191. https://doi.org/10.1186/s12885-015-1098-z.

An, R., Ji, M., Yan, H., Guan, C., 2018. Impact of ambient air pollution on obesity: A systematic review. Int. J. Obes. 42, 1112–1126. https://doi.org/10.1038/s41366-018-0089-y.

Antrop, M., 2000. Background concepts for integrated landscape analysis. Agric. Ecosyst. Environ. 77, 17–28. https://doi.org/10.1016/S0167-8809(99)00089-4.

Ascari, E., Licitra, G., Ancona, C., 2017. Noise pollution from road traffic noise in Rome: Incidence of coronary and cardiovascular events. J. Acoust. Soc. Am. 141, 3802. https://doi.org/10.1121/1.4988393.

Attademo, L., Bernardini, F., Garinella, R., Compton, M.T., 2017. Environmental pollution and risk of psychotic disorders: A review of the science to date. Schizophr. Res. 181, 55–59. https://doi.org/10.1016/j.schres.2016.10.003.

Babadjouni, R.M., Hodis, D.M., Radwanski, R., Durazo, R., Patel, A., Liu, Q., Mack, W.J., 2017. Clinical effects of air pollution on the central nervous system; a review. J Clin Neurosci 43, 16–24. https://doi.org/10.1016/j.jocn.2017.04.028.

Bernardini, F., Trezzi, R., Quartesan, R., Attademo, L., 2020. Air pollutants and daily hospital admissions for psychiatric care: A review. Psychiatr. Serv. 71, 1270–1276. https://doi.org/10.1176/appi.ps.201800565.

Besser, L.M., McDonald, N.C., Song, Y., Kukull, W.A., Rodriguez, D.A., 2017. Neighborhood Environment and Cognition in Older Adults: A Systematic Review. Am. J. Prev. Med. 53, 241–251. https://doi.org/10.1016/j.amepre.2017.02.013.

Beyer, K., Wallis, A.B., Hamberger, L.K., 2015. Neighborhood environment and intimate partner violence: a systematic review. Trauma. Violence Abuse 16, 16–47. https://doi.org/10.1177/1524838013515758.

Bogar, S., Beyer, K.M., 2016. Green Space, Violence, and Crime: A Systematic Review. Trauma. Violence Abuse 17, 160–171. https://doi.org/10.1177/1524838015576412.

Bonaccorsi, G., Milani, C., Giorgetti, D., Setola, N., Naldi, E., Manzi, F., Del Riccio, M., Dellisanti, C., Lorini, C., 2022. Impact of Built Environment and Neighborhood on Promoting Mental Health, Well-being, and Social Participation in Older People: an Umbrella Review. Ann, Ig 35, 213-239.https://dx.doi.org/10.7416/ai.2022.2534.

Bray, I., Reece, R., Sinnett, D., Martin, F., Hayward, R., 2022. Exploring the role of exposure to green and blue spaces in preventing anxiety and depression among young people aged 14–24 years living in urban settings: A systematic review and conceptual framework. Environ. Res. 214, 114081 https://doi.org/10.1016/j.envres.2022.114081.

Cabrera-Barona, P., Murphy, T., Kienberger, S., Blaschke, T., 2015. A multi-criteria spatial deprivation index to support health inequality analyses. Int. J. Health Geogr. 14, 1–14. https://doi.org/10.1186/s12942-015-0004-x.

Cardoso-dos-Santos, A.C., Boquett, J., Zagonel de Oliveira, M., Callegari-Jacques, S.M., Barbian, M.H., Sanseverino, M.T.V., Matte, U., Schuler-Faccini, L., 2018. Twin Peaks: A spatial and temporal study of twinning rates in Brazil. PLoS One 13, e0200885. https://doi.org/10.1371/JOURNAL.PONE.0200885.

Cartone, A., Postiglione, P., 2021. Principal component analysis for geographical data: the role of spatial effects in the definition of composite indicators. Spat. Econ. Anal. 16, 126–147. https://doi.org/10.1080/17421772.2020.1775876.

US CDC, 2022. PLACES: Local Data for Better Health [WWW Document]. URL https://www.cdc.gov/places/index.html.

Cesaroni, G., Porta, D., Badaloni, C., Stafoggia, M., Eeftens, M., Meliefste, K., Forastiere, F., 2012. Nitrogen dioxide levels estimated from land use regression models several years apart and association with mortality in a large cohort study. Environ. Health 11. https://doi.org/10.1186/1476-069X-11-48.

Cesaroni, G., Badaloni, C., Gariazzo, C., Stafoggia, M., Sozzi, R., Davoli, M., Forastiere, F., 2013. Long-Term Exposure to Urban Air Pollution and Mortality in a Cohort of More than a Million Adults in Rome. Environ. Health Perspect. 121, 324. https://doi.org/10.1289/EHP.1205862.

Chang, J.S., Brost, R.A., Isaksen, I.S.A., Madronich, S., Middleton, P., Stockwell, W.R., Walcek, C.J., 1987. A three-dimensional Eulerian acid deposition model: Physical concepts and formulation. J. Geophys. Res. 92, 14681–14700. https://doi.org/10.1029/JD092ID12P14681.

Chen, X., Lee, C., Huang, H., 2022. Neighborhood built environment associated with cognition and dementia risk among older adults: A systematic literature review. Soc. Sci. Med. 292, 114560 https://doi.org/10.1016/j.socscimed.2021.114560.

Dambha-Miller, H., Cheema, S., Saunders, N., Simpson, G., 2022. Multiple Long-Term Conditions (MLTC) and the environment: A scoping review. Int. J. Environ. Res. Public Health. 19, 11492. https://doi.org/10.3390/ijerph191811492.

De la Fuente, F., Saldias, M.A., Cubillos, C., Mery, G., Carvajal, D., Bowen, M., Bertoglia, M.P., 2021. Green space exposure association with type 2 diabetes mellitus, physical activity, and obesity: A systematic review. Int. J. Environ. Res. Public Health 18, 1–18. https://doi.org/10.3390/ijerph18010097.

Degbelo, A., Kuhn, W., 2018. Spatial and temporal resolution of geographic information: an observation-based theory. Open Geospatial Data, Softw. Stand. 2018 31 3, 1–22. https://doi.org/10.1186/S40965-018-0053-8.

Deguen, S., Zmirou-Navier, D., 2010. Social inequalities resulting from health risks related to ambient air quality–A European review. Eur. J. Public Health 20, 27–35. https://doi.org/10.1093/eurpub/ckp220.

Delmelle, E.M., Desjardins, M.R., Jung, P., Owusu, C., Lan, Y., Hohl, A., Dony, C., 2022. Uncertainty in geospatial health: challenges and opportunities ahead. Ann. Epidemiol. 65, 15–30. https://doi.org/10.1016/J.ANNEPIDEM.2021.10.002.

Demšar, U., Harris, P., Brunsdon, C., Fotheringham, A.S., McLoone, S., 2013. Principal Component Analysis on Spatial Data: An Overview. Ann. Assoc. Am. Geogr. 103, 106–128. https://doi.org/10.1080/00045608.2012.689236.

DenBraver, N.R., Lakerveld, J., Rutters, F., Schoonmade, L.J., Brug, J., Beulens, J.W.J., 2018. Built environmental characteristics and diabetes: A systematic review and meta-analysis. BMC Med. 16, 12. https://doi.org/10.1186/s12916-017-0997-z.

Dendup, T., Feng, X., Clingan, S., Astell-Burt, T., 2018. Environmental risk factors for developing type 2 diabetes mellitus: A systematic review. Int. J. Environ. Res. Public Health 15, 78. https://doi.org/10.3390/ijerph15010078.

Dzhambov, A.M., Dimitrova, D.D., 2018. Residential road traffic noise as a risk factor for hypertension in adults: Systematic review and meta-analysis of analytic studies published in the period 2011–2017. Environ. Pollut. 240, 306–318. https://doi.org/10.1016/j.envpol.2018.04.122.

Farchi, S., Forastiere, F., Vecchi Brumatti, L., Alviti, S., Arnofi, A., Bernardini, T., Bin, M., Brescianini, S., Colelli, V., Cotichini, R., Culasso, M., De Bartolo, P., Felice, L., Fiano, V., Fioritto, A., Frizzi, A., Gagliardi, L., Giorgi, G., Grasso, C., La Rosa, F., Loganes, C., Lorusso, P., Martini, V., Merletti, F., Medda, E., Montelatici, V., Mugelli, I., Narduzzi, S., Nisticò, L., Penna, L., Piscianz, E., Piscicelli, C., Poggesi, G., Porta, D., Ranieli, A., Rapisardi, G., Rasulo, A., Richiardi, L., Rusconi, F., Serino, L., Stazi, M.A., Toccaceli, V., Todros, T., Tognin, V., Trevisan, M., Valencic, E., Volpi, P., Ziroli, V., Ronfani, L., Di Lallo, D., 2014. Piccolipiù, a multicenter birth cohort in Italy: protocol of the study. BMC Pediatr. 14 https://doi.org/10.1186/1471-2431-14-36.

Tejedor-Flores, N., Vicente-Galindo, P., Galindo-Villardón, P., 2020. GEOGRAPHICALLY WEIGHTED PRINCIPAL COMPONENTS ANALYSIS APPROACH TO EVALUATE ELECTRICITY CONSUMPTION BEHAVIOUR. Sustain. City XIV. https://doi.org/10.2495/SC200091.

de'Donato, F., Leone, M., Stafoggia, M., Marino, C., Fabrizi, R., Michelozzi, P., 2018. Urban heat island and socio-economic position as factors that increase the risk of heat-related mortality in Rome, Italy (ISEE Conference Abstract). Environ. Health Perspect. 2011, 1. doi:10.1289/isee.2011.01134.

The Open Knowledge Foundation, 2023. Open Street map data [WWW Document]. website. URL https://www.openstreetmap.org/export#map=5/56.829/59.897.

Geneshka, M., Coventry, P., Cruz, J., Gilbody, S., 2021. Relationship between green and blue spaces with mental and physical health: A systematic review of longitudinal observational studies. Int. J. Environ. Res. Public Health 18, 9010. https://doi.org/10.3390/ijerph18179010.

Gollini, I., Lu, B., Charlton, M., Brunsdon, C., Harris, P., 2015. GWmodel: An R Package for Exploring Spatial Heterogeneity Using Geographically Weighted Models. J. Stat. Softw. 63, 1–50. https://doi.org/10.18637/JSS.V063.I17.

Harris, P., Brunsdon, C., Charlton, M., 2011. Geographically weighted principal components analysis. Int. J. Geogr. Inf. Sci. 25, 1717–1736. https://doi.org/10.1080/13658816.2011.554838.

Hu, C.Y., Yang, X.J., Gui, S.Y., Ding, K., Huang, K., Fang, Y., Jiang, Z.X., Zhang, X.J., 2021. Residential greenness and birth outcomes: A systematic review and meta-analysis of observational studies. Environ. Res. 193, 110599 https://doi.org/10.1016/j.envres.2020.110599.

Islam, M.Z., Johnston, J., Sly, P.D., 2020. Green space and early childhood development: a systematic review. Rev. Environ. Health 35, 189–200. https://doi.org/10.1515/reveh-2019-0046.

Italian National Institute for Environmental Protection, 2018. Corine Land Cover 2018 [WWW Document]. website. URL https://www.isprambiente.gov.it/it/attivita/biodiversita/documenti/corine-land-cover-clc (accessed 05.19.23).

Italian National Statistics Institute, 2011. 2011 General Population and Housing Census [WWW Document]. website. URL https://www.istat.it/it/censimenti-permanenti/censimenti-precedenti/popolazione-e-abitazioni/popolazione-2011.
Italian National Statistics Institute, 2022. Demography in numbers [Demografia in cifre] [WWW Document]. URL https://demo.istat.it/ (accessed 12.19.22).
Jia, P., Dai, S., Rohli, K.E., Rohli, R.V., Ma, Y., Yu, C., Pan, X., Zhou, W., 2021. Natural environment and childhood obesity: A systematic review. Obes. Rev. 22, e13097. https://doi.org/10.1111/obr.13097.
Johnson, K.A., Showell, N.N., Flessa, S., Janssen, M., Reid, N., Cheskin, L.J., Thornton, R. L.J., 2019. Do Neighborhoods Matter? A Systematic Review of Modifiable Risk Factors for Obesity among Low Socio-Economic Status Black and Hispanic Children. Child. Obes. 15, 71–86. https://doi.org/10.1089/chi.2018.0044.
Kabisch, N., van den Bosch, M., Lafortezza, R., 2017. The health benefits of nature-based solutions to urbanization challenges for children and the elderly - A systematic review. Environ. Res. 159, 362–373. https://doi.org/10.1016/j.envres.2017.08.004.
Kjellstrom, T., Friel, S., Dixon, J., Corvalan, C., Rehfuess, E., Campbell-Lendrum, D., Gore, F., Bartram, J., 2007. Urban Environmental Health Hazards and Health Equity. J. Urban Health 84, 86. https://doi.org/10.1007/S11524-007-9171-9.
Lallo, C., Raitano, M., 2018. Life expectancy inequalities in the elderly by socioeconomic status: evidence from Italy. Popul. Health Metr. 16 https://doi.org/10.1186/S12963-018-0163-7.
Lam, T.M., Vaartjes, I., Grobbee, D.E., Karssenberg, D., Lakerveld, J., 2021. Associations between the built environment and obesity: an umbrella review. Int. J. Health Geogr. 20, 7. https://doi.org/10.1186/s12942-021-00260-6.
Lee, K.J., Moon, H., Yun, H.R., Park, E.L., Park, A.R., Choi, H., Hong, K., Lee, J., 2020. Greenness, civil environment, and pregnancy outcomes: Perspectives with a systematic review and meta-analysis. Environ. Heal. A Glob. Access Sci. Source 19, 91. https://doi.org/10.1186/s12940-020-00649-z.
Lee, S. Il, 2001. Developing a bivariate spatial association measure: An integration of Pearson's r and Moran's I. J. Geogr. Syst. 2001 34 3, 369–385. https://doi.org/10.1007/S101090100064.
Li, M.H., Fan, L.C., Mao, B., Yang, J.W., Choi, A.M.K., Cao, W.J., Xu, J.F., 2016. Short-term exposure to ambient fine particulate matter increases hospitalizations and mortality in COPD: A systematic review and meta-analysis. Chest 149, 447–458. https://doi.org/10.1378/chest.15-0513.
Lin, C.Y., Hsu, C.Y., Gunnell, D., Chen, Y.Y., Chang, S.S., 2019. Spatial patterning, correlates, and inequality in suicide across 432 neighborhoods in Taipei City. Taiwan. Soc. Sci. Med. 222, 20–34. https://doi.org/10.1016/J.SOCSCIMED.2018.12.011.
Lloyd, C.D., 2010. Analysing population characteristics using geographically weighted principal components analysis: A case study of Northern Ireland in 2001. Comput. Environ. Urban Syst. 34, 389–399. https://doi.org/10.1016/J.COMPENVURBSYS.2010.02.005.
Lu, B., Harris, P., Charlton, M., Brunsdon, C., 2014. The GWmodel R package: further topics for exploring spatial heterogeneity using geographically weighted models. Geo-spatial Inf. Sci. 17, 85–101. https://doi.org/10.1080/10095020.2014.917453.
Luque-Garcia, L., Corrales, A., Lertxundi, A., Diaz, S., Ibarluzea, J., 2022. Does exposure to greenness improve children's neuropsychological development and mental health? A Navigation Guide systematic review of observational evidence for associations. Environ. Res. 206, 112599 https://doi.org/10.1016/j.envres.2021.112599.
Marinacci, C., Grippo, F., Pappagallo, M., Sebastiani, G., Demaria, M., Vittori, P., Caranci, N., Costa, G., 2013. Social inequalities in total and cause-specific mortality of a sample of the Italian population, from 1999 to 2007. Eur. J. Public Health 23, 582–587. https://doi.org/10.1093/EURPUB/CKS184.
Michelozzi, P., Fusco, D., Forastiere, F., Ancona, C., Dell'Orco, V., Perucci, C.A., 1998. Small area study of mortality among people living near multiple sources of air pollution. Occup. Environ. Med. 55, 611–615. https://doi.org/10.1136/OEM.55.9.611.
Min, E., Piazza, M., Galaviz, V.E., Saganic, E., Schmeltz, M., Freelander, L., Farquhar, S. A., Karr, C.J., Gruen, D., Banerjee, D., Yost, M., Seto, E.Y.W., 2021. Quantifying the Distribution of Environmental Health Threats and Hazards in Washington State Using a Cumulative Environmental Inequality Index. Environ. Justice 14, 298–314. https://doi.org/10.1089/ENV.2021.0021.
Mmako, N.J., Courtney-Pratt, H., Marsh, P., 2020. Green spaces, dementia and a meaningful life in the community: A mixed studies review. Heal. Place 63, 102344. https://doi.org/10.1016/j.healthplace.2020.102344.
National Toxicology, P., 2019. NTP monograph on the systematic review of traffic-related air pollution and hypertensive disorders of pregnancy. NTP Monogr. https://doi.org/10.22427/NTP-MGRAPH-7.
Nguyen, P.Y., Astell-Burt, T., Rahimi-Ardabili, H., Feng, X., 2021. Green space quality and health: A systematic review. Int. J. Environ. Res. Public Health 18, 11028. https://doi.org/10.3390/ijerph182111028.
Padeiro, M., de Sao Jose, J., Amado, C., Sousa, L., Roma Oliveira, C., Esteves, A., McGarrigle, J., 2022. Neighborhood Attributes and Well-Being Among Older Adults in Urban Areas: A Mixed-Methods Systematic Review. Res. Aging 44, 351–368. https://doi.org/10.1177/0164027521999980.
Padilla, C.M., Kihal-Talantikit, W., Vieira, V.M., Deguen, S., 2016. City-Specific Spatiotemporal Infant and Neonatal Mortality Clusters: Links with Socioeconomic and Air Pollution Spatial Patterns in France. Int. J. Environ. Res. Public Heal. 2016, Vol. 13, Page 624 13, 624. https://doi.org/10.3390/IJERPH13060624.
Lazio Region, Department of Epidemiology of Lazio Region, 2023. Opensalutelazio website [WWW Document]. Inferenze. URL https://www.opensalutelazio.it/salute/.
Ribeiro, A.I., De Fátima De Pina, M., Mitchell, R., 2015. Development of a measure of multiple physical environmental deprivation. After United Kingdom and New Zealand. Portugal. Eur. J. Public Health 25, 610–617. https://doi.org/10.1093/EURPUB/CKU242.
Richardson, E.A., Mitchell, R.J., Shortt, N.K., Pearce, J., Dawson, T.P., 2009. Evidence-based selection of environmental factors and datasets for measuring multiple environmental deprivation in epidemiological research. Environ. Heal. a Glob. access Sci. source 8 Suppl 1. https://doi.org/10.1186/1476-069X-8-S1-S18.
Richardson, E.A., Mitchell, R., Shortt, N.K., Pearce, J., Dawson, T.P., 2010. Developing Summary Measures of Health-Related Multiple Physical Environmental Deprivation for Epidemiological Research. Environ. Plan. A Econ. Sp. 42, 1650–1668. https://doi.org/10.1068/A42459.
Rojas-Rueda, D., Morales-Zamora, E., Alsufyani, W.A., Herbst, C.H., AlBalawi, S.M., Alsukait, R., Alomran, M., 2021. Environmental risk factors and health: An umbrella review of meta-analyses. Int. J. Environ. Res. Public Health 18, 1–38. https://doi.org/10.3390/ijerph18020704.
Rosano, A., Pacelli, B., Zengarini, N., Costa, G., Cislaghi, C., Caranci, N., 2020. Update and review of the 2011 Italian deprivation index calculated at the census section level. Epidemiol. Prev. 44, 162–170. https://doi.org/10.19191/EP20.2-3.P162.039.
Rugel, E.J., Brauer, M., 2020. Quiet, clean, green, and active: A Navigation Guide systematic review of the impacts of spatially correlated urban exposures on a range of physical health outcomes. Environ. Res. 185, 109388 https://doi.org/10.1016/j.envres.2020.109388.
Saib, M.S., Caudeville, J., Beauchamp, M., Carré, F., Ganry, O., Trugeon, A., Cicolella, A., 2015. Building spatial composite indicators to analyze environmental health inequalities on a regional scale. Environ. Health 14. https://doi.org/10.1186/S12940-015-0054-3.
Salgado, M., Madureira, J., Mendes, A.S., Torres, A., Teixeira, J.P., Oliveira, M.D., 2020. Environmental determinants of population health in urban settings. A systematic review. BMC Public Health 20, 853. https://doi.org/10.1186/s12889-020-08905-0.
Samoli, E., Stergiopoulou, A., Santana, P., Rodopoulou, S., Mitsakou, C., Dimitroulopoulou, C., Bauwelinck, M., de Hoogh, K., Costa, C., Marí-Dell'Olmo, M., Corman, D., Vardoulakis, S., Katsouyanni, K., 2019. Spatial variability in air pollution exposure in relation to socioeconomic indicators in nine European metropolitan areas: A study on environmental inequality. Environ. Pollut. 249, 345–353. https://doi.org/10.1016/J.ENVPOL.2019.03.050.
Sartorius, B.K.D., Sartorius, K., 2014. A new multidimensional population health indicator for policy makers: absolute level, inequality and spatial clustering - an empirical application using global sub-national infant mortality data. Geospat. Health 9, 7–26. https://doi.org/10.4081/GH.2014.2.
Schuurman, N., Bell, N., Dunn, J.R., Oliver, L., 2007. Deprivation Indices, Population Health and Geography: An Evaluation of the Spatial Effectiveness of Indices at Multiple Scales. J. Urban Heal. 2007 844 84, 591–603. https://doi.org/10.1007/s11524-007-9193-3.
Slachtova, H., Jirik, V., Tomasek, I., Tomaskova, H., 2016. Environmental and Socioeconomic Health Inequalities: a Review and an Example of the Industrial Ostrava Region. Cent. Eur. J. Public Health 24, S26–S32. https://doi.org/10.21101/cejph.a4535.
Soffian, S.S.S., Nawi, A.M., Hod, R., Chan, H.K., Hassan, M.R.A., 2021. Area-level determinants in colorectal cancer spatial clustering studies: A systematic review. Int. J. Environ. Res. Public Health 18, 10486. https://doi.org/10.3390/ijerph181910486.
Sokale, I.O., Conway, S.H., Douphrate, D.I., 2022. Built Environment and Its Association with Depression among Older Adults: A Systematic Review. Open Public Health J. 15 https://doi.org/10.2174/18749445-v15-e2202030 e187494452202030.
Stieb, D.M., Zheng, C., Salama, D., Berjawi, R., Emode, M., Hocking, R., Lyrette, N., Matz, C., Lavigne, E., Shin, H.H., 2020. Systematic review and meta-analysis of case-crossover and time-series studies of short term outdoor nitrogen dioxide exposure and ischemic heart disease morbidity. Environ. Heal. A Glob. Access Sci. Source 19, 47. https://doi.org/10.1186/s12940-020-00601-1.
Sui, Y., Ettema, D., Helbich, M., 2022. Longitudinal associations between the neighborhood social, natural, and built environment and mental health: A systematic review with meta-analyses. Heal. Place 77, 102893. https://doi.org/10.1016/j.healthplace.2022.102893.
Tobler, W.R., 1970. A Computer Movie Simulating Urban Growth in the Detroit Region. Econ. Geogr. 46, 234. https://doi.org/10.2307/143141.
Tobler, W., 2004. On the First Law of Geography: A Reply. Ann. Assoc. Am. Geogr. 94, 304–310. https://doi.org/10.1111/j.1467-8306.2004.09402009.x.
Tortorella, A., Menculini, G., Moretti, P., Attademo, L., Balducci, P.M., Bernardini, F., Cirimbilli, F., Chieppa, A.G., Ghiandai, N., Erfurth, A., 2022. New determinants of mental health: the role of noise pollution. A narrative review. Int. Rev. Psychiatry. https://doi.org/10.1080/09540261.2022.2095200.
United Nations, 2022a. The Sustainable Development Goals Report 2022.[WWW Document] URL: https://unstats.un.org/sdgs/report/2022/ (accessed 05.19.23).
United Nations, 2022b. World Cities Report 2022: Envisaging the Future of Cities. Nairobi, Kenya.[WWW Document]. URL: https://unhabitat.org/world-cities-report-2022-envisaging-the-future-of-cities (accessed 05.19.23).
van den Bosch, M., Ode Sang, Å., 2017. Urban natural environments as nature-based solutions for improved public health – A systematic review of reviews. Env. Res 158, 373–384. https://doi.org/10.1016/j.envres.2017.05.040.
Vanaken, G.J., Danckaerts, M., 2018. Impact of green space exposure on children's and adolescents' mental health: A systematic review. Int. J. Environ. Res. Public Health 15, 2668. https://doi.org/10.3390/ijerph15122668.
Vilcassim, M.J.R., Callahan, A.E., Zierold, K.M., 2021. Travelling to polluted cities: a systematic review on the harm of air pollution on international travellers' health. J. Travel Med. 28 https://doi.org/10.1093/jtm/taab055.
Waidyatillake, N.T., Campbell, P.T., Vicendese, D., Dharmage, S.C., Curto, A., Stevenson, M., 2021. Particulate matter and premature mortality: A Bayesian meta-

analysis. Int. J. Environ. Res. Public Health 18, 7655. https://doi.org/10.3390/ijerph18147655.
Wimalasena, N.N., Chang-Richards, A., Wang, K.I.K., Dirks, K.N., 2021. Housing risk factors associated with respiratory disease: A systematic review. Int. J. Environ. Res. Public Health 18, 1–26. https://doi.org/10.3390/ijerph18062815.
World Health Organization, 2022. WHO Repository of urban health resources [WWW Document]. URL https://urbanhealth-repository.who.int/ (accessed 12.15.22).
Xu, Z., FitzGerald, G., Guo, Y., Jalaludin, B., Tong, S., 2016. Impact of heatwave on mortality under different heatwave definitions: A systematic review and meta-analysis. Environ. Int. 89–90, 193–203. https://doi.org/10.1016/j.envint.2016.02.007.
Xu, Z., Crooks, J.L., Davies, J.M., Khan, A.F., Hu, W., Tong, S., 2018. The association between ambient temperature and childhood asthma: a systematic review. Int. J. Biometeorol. 62, 471–481. https://doi.org/10.1007/s00484-017-1455-5.
Yang, L., Zhang, H., Zhang, X., Xing, W., Wang, Y., Bai, P., Zhang, L., Hayakawa, K., Toriba, A., Tang, N., 2021. Exposure to atmospheric particulate matter-bound polycyclic aromatic hydrocarbons and their health effects: A review. Int. J. Environ. Res. Public Health 18, 1–25. https://doi.org/10.3390/ijerph18042177.
Ye, T., Yu, P., Wen, B., Yang, Z., Huang, W., Guo, Y., Abramson, M.J., Li, S., 2022. Greenspace and health outcomes in children and adolescents: A systematic review. Environ. Pollut. 314, 120193 https://doi.org/10.1016/j.envpol.2022.120193.
Zhang, Y., van Dijk, T., Yang, Y., 2022. Green place rather than green space as a health determinant: A 20-year scoping review. Environ. Res. 214, 113812 https://doi.org/10.1016/j.envres.2022.113812.
Zhu, R.X., Nie, X.H., Chen, Y.H., Chen, J., Wu, S.W., Zhao, L.H., 2020. Relationship Between Particulate Matter (PM2.5) and Hospitalizations and Mortality of Chronic Obstructive Pulmonary Disease Patients: A Meta-Analysis. Am. J. Med. Sci. 359, 354–364. https://doi.org/10.1016/j.amjms.2020.03.016.